Field-induced texture transitions in a bent-core nematic liquid crystal

R. Stannarius,[1] A. Eremin,[1] M.-G. Tamba,[2] G. Pelzl,[2] and W. Weissflog[2]
[1]*Institute of Experimental Physics, Otto-von-Guericke-University, Universitätsplatz 2, D-39106 Magdeburg, Germany*
[2]*Institute of Physical Chemistry, Martin-Luther-University Halle, Mühlpforte 1, D-06108 Halle, Germany*
(Received 3 December 2006; revised manuscript received 2 November 2007; published 26 December 2007)

It is demonstrated in electro-optic experiments that an external electric field of the order of 10^5 V/m induces persisting texture transitions in a nematic phase formed by bent-core mesogens. The field-induced metastable state is identified by its optical and electric properties. After the field is switched off, the original and induced states can coexist in domains for about one hour in planar sandwich cells. During this time, the induced domains gradually shrink but they can be stabilized in moderate electric fields. The occurrence of similar domains in homeotropic cells suggests that the transition into a metastable biaxial state is observed. In the field-free planar ground state, the formation of inversion walls is observed inside the metastable domains.

DOI: 10.1103/PhysRevE.76.061704 PACS number(s): 64.70.Md, 61.30.Gd

I. INTRODUCTION

Bent-shaped mesogens are known to exhibit numerous liquid crystalline mesophases, including many layered and columnar structures [1]. For sterical reasons, they are less suited to form a nematic phase; the bent shape of the molecules favors layered or other positional packing. Nevertheless, several successful strategies to produce nematic phases of bent-core mesogens have been reported [1–7]. The tendency for molecular positional order is smaller, for example, when the bending angle of the "banana-shaped" molecule is increased toward a stretched angle by lateral substituents at the central phenyl ring [1]. Nematic phases are also found in mixtures of calamitic and bent-core mesogens [2]. The material studied here is a twin mesogen with a bent-core subunit covalently bound to a rodlike part by a flexible spacer [7]; its chemical structure is shown in Fig. 1.

In smectic phases formed by bent core mesogens, electric fields can induce structural changes, for example, the switching of the phase chirality. Domains of different chirality can coexist, and switching processes may even compete in one sample, e.g., one preserving the chirality of the molecular arrangement and the second converting it [8], depending on temperature and frequency, but also on the applied field strength. Domains of opposite chirality may grow or shrink in dependence on the direction of the applied electric field, and even the phase transition from the isotropic phase into a mesophase with spontaneous polarization may be reversibly controlled by means of electric fields [9,10]. Nematic phases, owing to the absence of long range positional order, are characterized by additional degrees of freedom of the director $\hat{n}$. Consequently, one finds other prominent influences of the bent-core molecular geometry on physical properties, in both quantitative and qualitative aspects. An example is the discovery of a giant bend flexoelectric coefficient e_{33} in a bent-core nematic [11]. Unconventional types of electrically driven convection structures have been described [12,13]. The electro-optic behavior of sandwich cells filled with bent-core nematics is substantially different from that of calamitic nematics [14].

Their sterical shapes qualify bent-core nematogens as potential candidates for biaxial order. Biaxial nematic phases have been long sought with little success in calamitic thermotropic materials. Since the discovery of biaxial lyotropic nematics [15], there have been numerous efforts to find biaxiality in thermotropic nematics, using a variety of experimental techniques. Finally, biaxial nematics of bent-core mesogens have been identified by NMR and x-ray methods [16–18].

The purpose of this paper is to present evidence from electro-optical experiments that, in a sufficiently strong external electric field, one can transform the uniaxial phase of the mesogen in Fig. 1 into a metastable biaxial state, either in the complete cell or in domains coexisting with domains in the original uniaxial state. By studying planar and homeotropic cells, we provide arguments that this biaxial state is not simply imposed by boundary conditions of the cell but appears to be a biaxial, thermodynamically metastable nematic phase.

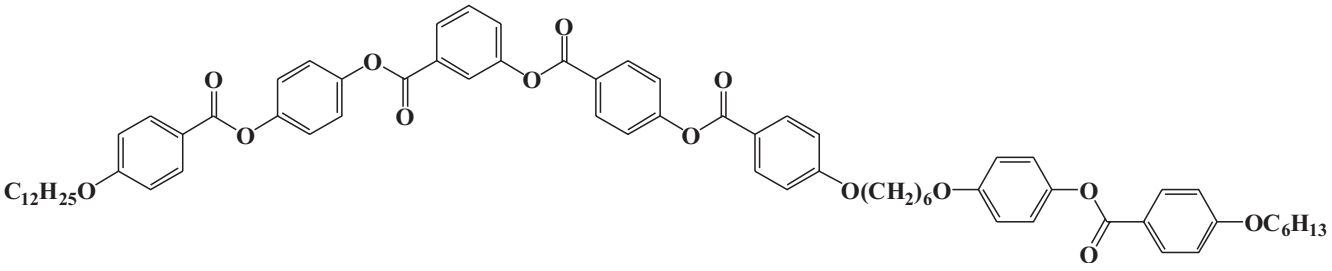

FIG. 1. Chemical structure of the investigated mesogen. The phase sequence is Cr 160 (SmC 149) N 167.5 I [7].

II. MATERIAL AND EXPERIMENTAL SETUP

We use a commercial sandwich cell (E.H.C.) with a cell gap of $d=25\ \mu$m and rubbed polyimide coating of the glass plates for planar surface alignment. The cell is observed in transmission with a high-resolution cooled CCD camera AxioCam HR mounted on an AxioImager polarizing microscope (Carl Zeiss GmbH). All experiments are performed in monochromatic light ($\lambda=532$ nm), between crossed polarizers (vertical and horizontal in the images). Temperature is controlled with a Linkam LTS 350 heating stage. If not otherwise indicated, data refer to a temperature 7.5 K below the clearing point T_{NI}. The ac voltages (1 kHz) are synthesized with a TGA 1241 (TTi) function generator and a broadband amplifier.

III. EXPERIMENTS IN PLANAR CELLS

We start with a model-free description of the experimental findings. The available amount of material was too small to measure dielectric constants or refractive indices, but the splay Fréedericksz transition (FT) evidences that the dielectric anisotropy $\Delta\varepsilon=\varepsilon_{\parallel}-\varepsilon_{\perp}$ is positive [14]. The sharp Fréedericksz threshold evidences that the surface alignment is good and the pretilt angle of the material can be neglected. From the FT threshold and the electro-optic characteristics above threshold, it has been possible to obtain information on the ratio of elastic constants and on the ratio between the dielectric anisotropy and the elastic splay constant. In Ref. [14], the material was investigated in its original state, which has the appearance of a uniaxial nematic phase, and which will henceforth be referred to as N_u.

The study of the splay FT in an electric field applied normal to the glass substrate [19] revealed the following unexpected effect: When the applied field strength is sufficiently large (a few hundred kV/m to 1 MV/m), a transition into a new state of order takes place, which after the removal of the field leads to an altered ground state. This second ground state differs optically from the planar ground state of the original, uniaxial nematic phase N_u. The so far unidentified new state is designated here preliminarily as N_b. It has the following fundamental properties: The direction of the largest refractive index of N_b in the cell plane is unchanged with respect to the optic axis of N_u in the planar cell (rubbing direction). With polarizers crossed parallel and perpendicular to the rubbing direction of the cell, both N_u and N_b states appear almost black. Under crossed polarizers diagonal to the director easy axis, the two states are easily distinguished by the change of birefringence. The effective birefringence in the off state is reduced by about 15%. With a compensator we measure a drop of $\Delta n=n_e-n_o=0.136$ in N_u to $\Delta n'=\Delta n-\delta n=n_1-n_2=0.115$ in N_b. Here, n_e and n_o are extraordinary and ordinary refractive indices of N_u, while n_1, n_2 are the corresponding effective refractive indices in N_b, for normally incident light polarized $\parallel$ and $\perp$ to the alignment axis, respectively.

It is possible to transform the complete region under the cell electrodes into the new state, but one can also obtain textures where N_u and N_b domains coexist, as shown in Figs. 2–4. These domains are separated by sharp borders which have not the appearance of walls but of either defect lines or phase boundaries. In such situations, the N_b domains shrink slowly when the electric field is off. After approximately one hour, the uniform N_u ground state is reestablished in the

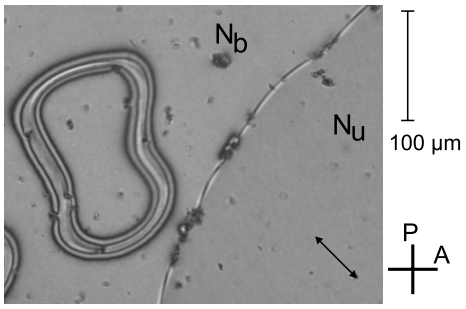

FIG. 2. Two coexisting domains in the N_b (left) and N_u (right) planar ground states at zero field. The N_b domain contains a wall structure in the form of a closed loop. The director easy axis $\hat{n}$ is in the direction of the arrow.

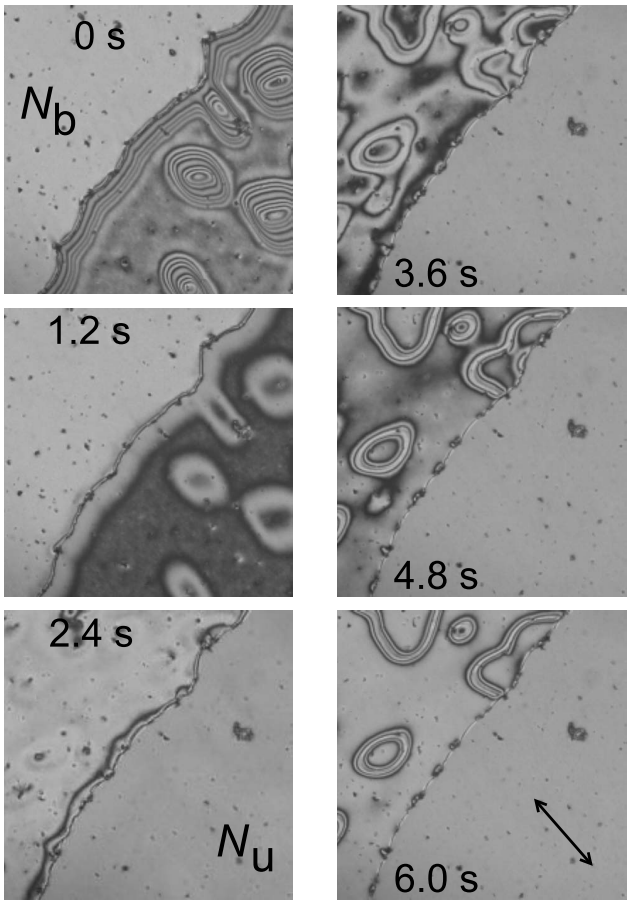

FIG. 3. Same domains as in the previous figure after a voltage of 7.35 V has been switched off. The images are taken in 1.2 s intervals. In the N_u domain (bottom right), the BL walls disappear and the sample relaxes to the all-planar state while in the N_b domain (top left) a new type of wall appears in the off state. Image sizes 546 μm $\times$ 546 μm.

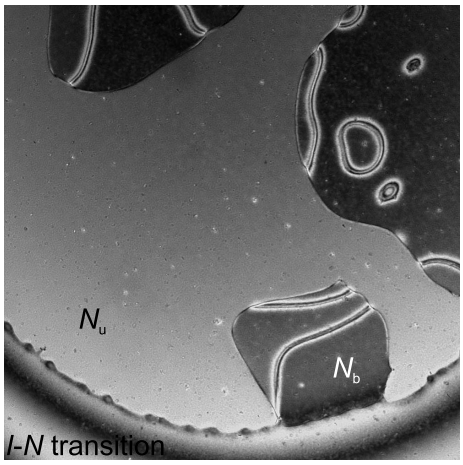

FIG. 4. N_u and N_b domains directly at the phase transition into the isotropic phase. In the field-free state shown, the N_u domain is uniform and the N_b domain contains stationary wall structures. In the bottom part of the image, the progressing nematic-isotropic phase boundary is seen. Image size 546 μm$\times$546 μm.

whole cell. One can, however, reverse the regression of N_b domains by applying a sufficiently strong electric field. At a few hundred MV/m, there is a clear progression of *existing* N_b domains.

It is a mere coincidence that both states appear almost equally bright at 7.5 K below T_{NI} (Fig. 2), the order of interference being 6.4 and $\approx$5.4, respectively. At other temperatures, the ratio of Δn to $\Delta n'$ remains approximately the same, so that at about 0.5 K below T_{NI}, N_u domains are near to a transmission maximum (half integer order $\Delta n d/\lambda$) while N_b domains are close to a minimum (integer $\Delta n' d/\lambda$). Figure 4 shows the cell directly at the nematic-isotropic transition. At that temperature, N_u appears bright, and N_b domains appear dark. The bottom part of the image shows the front of the phase transition.

N_b domains often contain walls in the off state (Figs. 2–4), in contrast to N_u domains which always relax to a uniform planar texture even if Brochard-Leger (BL) walls [20] had formed during the FT. This is seen in the image sequence in Fig. 3. The walls in the N_b field-off state have widths that are nearly independent of their orientations. This distinguishes them from the BL walls [14] in N_u above the Fréedericksz threshold. Moreover, they appear when the cell is switched off, irrespective of whether the tilted state above the FT was uniform or not (Fig. 3), and they disappear again above the Fréedericksz threshold. The walls often form closed loops that shrink on the time scale of minutes. Sometimes they are pinned with their ends at the borders of the N_b domain; then they may persist during the lifetime of the domain (Fig. 4). Their optical profile at 7.5 K below T_{NI} consists of four dark zones, separating bright zones. Optical textures on both wall sides are indistinguishable under crossed diagonal polarizers.

Figure 5 sketches schematically the state diagram of N_u in the 25 μm cell in the field strength and frequency parameter space. The FT has the lowest threshold, nearly frequency-independent. Above, there is a transition into a periodically

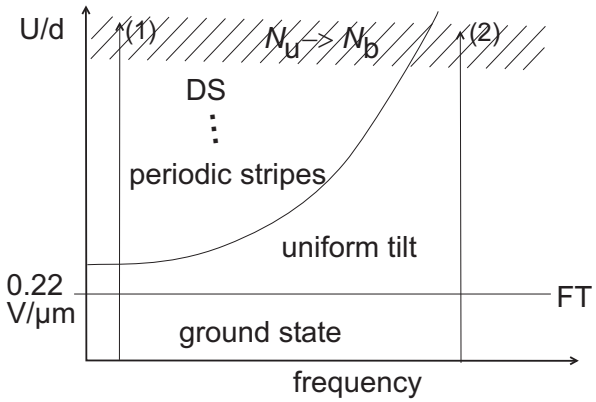

FIG. 5. Schematic sketch of the N_u orientational states in a 25 μm cell in the voltage-frequency space. The transition to N_b is indicated. Arrows (1), (2) are explained in the text.

distorted state, formed by electrically driven convection [13] and, after further instabilities, into a dynamic scattering (DS) regime. Details of the electro-optic characteristics of N_u are described in Refs. [13,14]. A similar behavior is found in N_b domains, but the thresholds in both states differ from each other. If one chooses path (1), the transition $N_u \rightarrow N_b$ appears in the turbulent DS pattern and the transformation itself is difficult to identify. Varying the field along path (2), one can observe the nucleation of N_b domains, preferentially inside BL walls.

Fringes in the optical profile of the original BL wall, Fig. 6(a), evidence the continuous director rotation across the wall [14,20] in the original N_u state. The change seen in the wall center in Fig. 6(b) reflects the transformation into an N_b domain, which later expands into adjacent N_u areas [Figs.

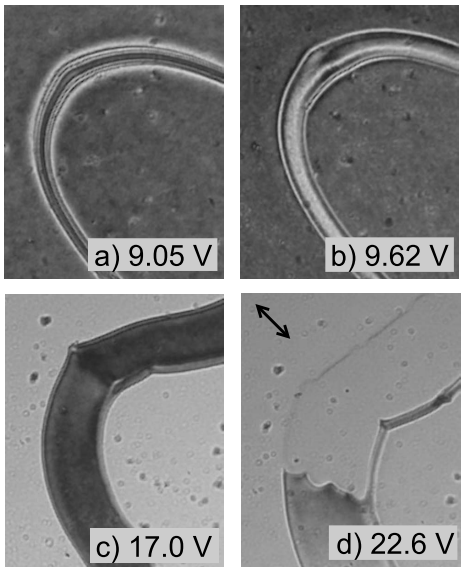

FIG. 6. (a) Texture of a BL wall in the N_u phase at 9.05 V. (b) An N_b domain is formed inside the wall at a voltage of 9.62 V (0.385 MV/m). (c), (d) The N_b domain has formed and expands into the surrounding N_u regions. Image sizes 106 μm$\times$132 μm and $T=T_{\mathrm{NI}}-0.5$ K.

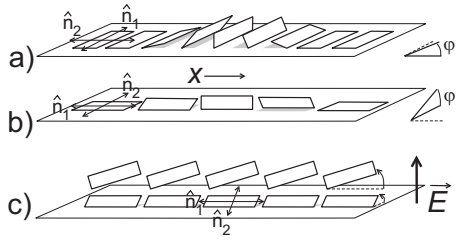

FIG. 7. Sketch of the two types of inversion walls of the second director $\hat{n}_2$ in the biaxial phase in a cell with strong planar anchoring of $\hat{n}_1$ and weak anchoring for $\hat{n}_2$. (a) Splay-bend wall, $\hat{n}_1 \perp x$; (b) twist wall, $\hat{n}_1 \| x$. (c) Alignment of $\hat{n}_2$ and FT of $\hat{n}_1$ in an electric field.

6(c) and 6(d)]. The boundaries between the two domains become sharp, the director field being discontinuous. The N_u and N_b domains have coincidently the same transmission intensity in Fig. 6(d), but they are in different interference maxima.

IV. DISCUSSION OF THE PLANAR CELL EXPERIMENTS

There may be different interpretations of these experimental observations; anchoring transitions cannot be excluded *a priori*. Another possible explanation is the assumption that the electric field induces a transition into a biaxial nematic phase N_b that is metastable at zero electric field. It is not excluded that the planar substrate contributes to a stabilization of the N_b state.

With this assumption, the basic optical properties of the induced domains can be explained as follows: The material is in an undistorted ground state when the field is switched off. Absolute values of the refractive indices of N_b are not available so far, but if one assumes that essentially the axes perpendicular to the first director are ordered, it is reasonable to assume that N_b has an unchanged refractive index $n_1 \approx n_e$ (along the first director, $\hat{n}_1$), and two different indices $n_2 = n_o + \delta_n$, and $n_3 = n_o - \delta_n$ (along the vertical axes $\hat{n}_2$, $\hat{n}_3$). If one assumes, e.g., $n_o = 1.5$, the corresponding values are $n_1 = 1.636$, $n_2 = 1.521$, and $n_3 = 1.479$. This yields an angle between the two optical axes of 66°, and a comparably large optical biaxiality, with $2\delta n = (n_2 - n_3) = 0.042$.

In N_b, the first director $\hat{n}_1$ is strongly anchored at the cell plates in rubbing direction (easy axis of the director in N_u). The second director $\hat{n}_2$ is weakly anchored planarly, perpendicular to $\hat{n}_1$. When the electric field is switched off, the first director relaxes to the all-planar undistorted state, while $\hat{n}_2$ is planar within domains that are separated by $\hat{n}_2$ inversion walls (Figs. 2–4). Their segments can be classified into $\hat{n}_2$ splay-bend and $\hat{n}_2$ twist types (Fig. 7). Wall segments that extend along the first director (in Fig. 2 top right and bottom left sectors in the loop seen) contain predominantly splay and bend of $\hat{n}_2$ [Fig. 7(a)], while wall segments perpendicular to the first director (top left and bottom right in Fig. 2) essentially contain twist of the second director [Fig. 7(b)]. For a calculation of the wall profiles, one-constant approximation that neglects the elastic anisotropy is a reasonable first estimate. It leads to the ansatz for the free energy per cell area

$$f = \frac{1}{2} K d (d\varphi/dx)^2 - W \sin^2 \varphi,$$

with the coordinate x perpendicular to the wall, the tilt angle φ of $\hat{n}_2$, the surface anchoring energy $\frac{1}{2} W \sin^2 \varphi(x)$, and an elastic constant K for $\hat{n}_2$. We assume that there is no variation of $\hat{n}_2$ normal to the cell plane in the off state. One obtains the solution

$$\varphi = 2 \arctan[\exp(x/\xi)] \quad \text{with} \quad \xi = \sqrt{Kd/(2W)}.$$

This corresponds to a ratio $K/W \approx (25 \pm 5)$ μm. If the anchoring of $\hat{n}_2$ were strong, one would find a pair of disclination lines at the glass substrates instead of the continuous wall.

However, this model of the $\hat{n}_2$ inversion walls [Figs. 7(a) and 7(b)] is only a crude estimate, since a more detailed analysis of the walls in polarized light reveals more complex optical characteristics. With the polarizer parallel to the rubbing direction, the minimum extinction appears when the analyzer is slightly rotated out of the crossed position. This means that the observed walls must actually have a more complex internal structure, and they also contain some deflections of the first director out of the planar orientation.

When an electric field is applied, the second director aligns toward $\vec{E}$ as shown in Fig. 7(c), and the walls disappear. Two reorientation processes take place concurrently: The rotation of $\hat{n}_2$ into the normal direction and the FT of $\hat{n}_1$. It is important to mention that the N_b domain has a sharp Fréedericksz threshold, as well as N_u. The FT threshold field in N_b is reduced by a factor of approximately 2 respective to N_u. When we assume that the splay constant for the first director is unchanged, an effective dielectric anisotropy $\varepsilon_\| - \varepsilon_{33}$ increased by this factor respective to $\Delta\varepsilon$ can explain the threshold drop [26]. Above the FT, the characteristics of N_b and N_u are comparable, when the voltages are scaled appropriately. Inversion walls of $\hat{n}_2$ in N_u disappear in the tilted director field, but they reappear at random positions when the field is switched off and the first director $\hat{n}_1$ relaxes to planar configuration again (Fig. 3).

The model can also explain why the transition $N_u \rightarrow N_b$, path (2) in Fig. 5, occurs first in BL wall centers. There, the director $\hat{n}$ remains planar, i.e., perpendicular to the field $\vec{E}$, even at high voltages [14] and consequently the electric forces acting toward an induction of order of the second axis are most effective.

After its nucleation, the N_b domain is surrounded by a sharp border, a phase boundary. Between the two domains, the director field is not continuous [Figs. 6(b)–6(d)]. The fringes that evidence a continuous deformation of the $\hat{n}$ director across the original BL wall [14,20] disappear. The N_b domain switches into a highly tilted state, where the first director $\hat{n}_1$ tilts toward $\vec{E}$ so that $\hat{n}_2$, $\hat{n}_3$ tilt away from $\vec{E}$. The ordering influence of the electric field on the second director $\hat{n}_2$ thus slightly decreases, but nevertheless the N_b domain, once nucleated, grows at the expense of the adjacent uniform N_u region.

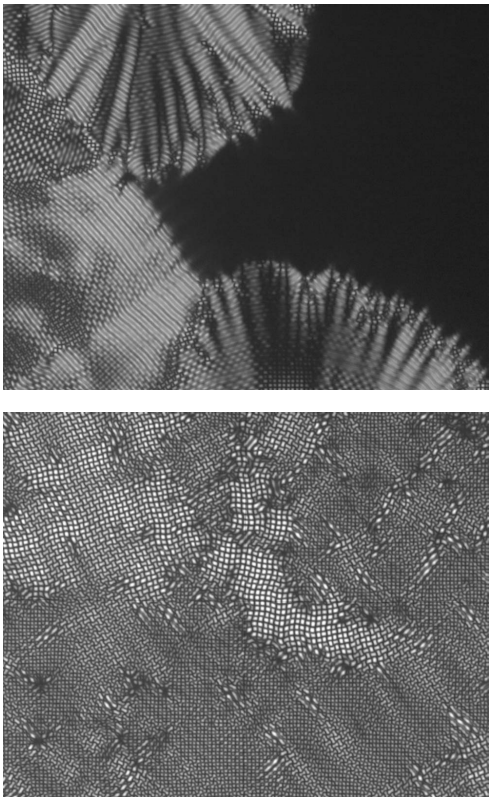

FIG. 8. Top: Onset of electroconvection in a 5 μm thick homeotropic cell. Bottom: Fully developed electroconvection pattern at 1 kHz ac excitation. The image size is 692 μm$\times$548 μm.

When the transformation occurs in the turbulent DS state [path (1) in Fig. 5], the director is randomly oriented. The electric field induces the N_b state in random domains that grow by coalescence. The threshold for the initiation of the N_b state is difficult to detect there but is apparently higher than along path (2).

V. EXPERIMENTS IN HOMEOTROPIC CELLS

In order to exclude other possible mechanisms that could lead to a change of the birefringence of the ground state, we have performed additional experiments in homeotropic cells. The two states N_u and N_b are observed there as well. The material has been filled into a 5 μm sandwich cell with homeotropic alignment conditions. In such a cell, the director $\hat{n}$ is initially in field direction; the sample is completely black between crossed polarizers in the N_u phase. In that geometry, the electric field applied normal to the glass plates cannot align the second director; one needs a mechanism that tilts the director out of the normal orientation first. For that purpose, we take advantage of the fact that, at high electric fields, electrically driven convection patterns are formed in the homeotropic cell. This situation is typical for material with negative conductivity anisotropy and positive dielectric anisotropy [21]. Figure 8 shows the onset of an electroconvection pattern (top) and the fully developed convection pattern in the cell. As well as in the planar case, the pattern

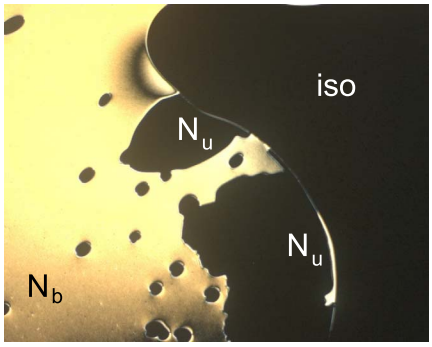

FIG. 9. (Color online) Texture at zero electric field, after application of a strong ac field (10 MV/m, 1 kHz) in a 5 μm homeotropic cell, white light illumination. The region in the right-hand part has undergone a nematic-isotropic transition. The region N_b is characterized by a bright Schlieren texture. Dark spots inside this area represent small domains of the N_u phase. The temperature is between T_{NI} and $T_{NI}-7.5$ K. Image size 692 μm$\times$548 μm.

undergoes a transition to a dynamic scattering state at higher voltages. When electric fields above 10 MV/m are applied, a similar transition to N_b as in the planar case is observed. The problem with this experiment is that it cannot be performed under isothermal conditions. Since the electroconvection pattern is highly dissipative, the cell heats up during the high-field application. When the field is suddenly switched off after a few seconds, the sample temperature is already close to the clearing point. The electroconvection pattern breaks down immediately after the field is off. This leaves the sample in a state similar to that shown in Fig. 9. This image shows a part of the cell in the isotropic phase (right), another part of the cell in the homeotropic biaxial nematic state (left), and domains of the homeotropic uniaxial nematic state (near the NI phase boundary and in the small circular spots). The N_u domains are black in the field off state, while the N_b domains are characterized by a bright Schlieren texture of the second director (Figs. 9 and 10).

If one uses the optical parameters that have been calculated from the birefringence of the planar cell in the ground state, the calculated interference order $(n_2-n_3)d/\lambda$ for the

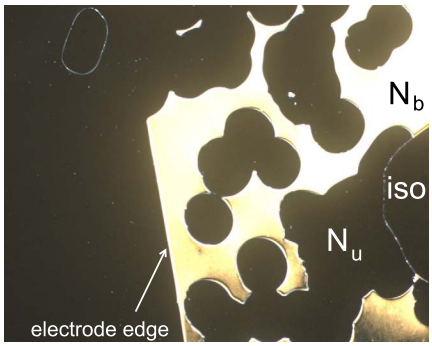

FIG. 10. (Color online) Biaxial nematic domain N_b in a 5 μm homeotropic cell, with enclosed circular domains of the uniaxial N_u phase, image size 692 μm$\times$548 μm. Outside the electrode area (left in the image), the sample is still N_u. The temperature is between T_{NI} and $T_{NI}-7.5$ K.

5 μm homeotropic cell is near the first maximum. This agrees very well with the observation in Figs. 9 and 10.

Apparently, the second director in N_b is hardly aligned by the lateral phase boundaries, but it varies slightly across the cell plane. Inversion walls of the second director appear as Schlieren in the top central part and at the bottom of Fig. 9. In the field-off state, the cell cools rapidly to the original temperature 7.5 K below the clearing point, and the isotropic phase retreats. At the same time, the N_u domains grow inside the N_b domain; after approximately 1 min, they cover the whole cell. A momentary picture of the growing N_u domains is seen in Fig. 10. This figure also shows the edge of the electrode area in the left-hand part. Outside the electrode area, no transition has taken place. The biaxial domain is only formed in the region of the electrodes.

VI. CONCLUSIONS AND SUMMARY

The observation of metastable, optically biaxial domains in the homeotropic cell and of domains with reduced birefringence in planar cells can be explained by a field-induced transition from a uniaxial into a biaxial nematic state. It is stabilized in moderate (<1 MV/m) fields. Other interpretations, like anchoring transitions leading to a deformed ground state, could possibly describe some aspects of the observations, in particular in the planar cell, but they fail to explain the combined results in planar and homeotropic cells.

At the present state, we have no experimental evidence whether the second director axis is polar or not. The molecular shape would suggest a polar ordering. This could not be tested in our ac electric field experiments. Studies with dc fields may solve this question, but so far the onset of strong convective flow at dc excitation prevented a reliable experimental data evaluation.

We emphasize that an ordering effect of the electric field on the short axes of the individual mesogens can be excluded. The interaction energy with individual molecules is far below thermal energy. However, we assume that there exist cybotactic clusters of mesogens with short range biaxial order. Owing to a random orientation of the second axis of these clusters, biaxiality averages out in the uniaxial phase. Only after application of the electric field, those collective clusters of mesogens are aligned to form a state with macroscopical biaxial order. We consider this property to form clusters with biaxial order in the uniaxial nematic phase a prerequisite for the observed effect; it is a unique property of bent-core mesogens like those used in our experiment. A similar idea has been proposed recently by Vanakaras and Photinos [22]; they consider different types of nematic phases of bent-core mesogens, including a true biaxial nematic phase N_b, a uniaxial phase N_u without biaxial clusters, and a uniaxial phase that contains biaxial clusters with disordered second axis.

The biaxially ordered phase persists after the field is removed, but it is metastable; the uniaxial phase is energetically preferred in the field-free state. A transition back into the uniaxial state occurs via nucleation of small uniaxial domains and growth of the uniaxial domains by the propagation of phase boundaries.

We finally discuss some conditions for the appearance of the N_b state. The mesogens have to be sufficiently flat, but smectic order has to be absent. The bent-core unit of the twin mesogen is sufficiently anisotropic to match the first condition, and the twin structure with a rodlike subunit reduces the tendency to form smectic layers. A special feature of the mesogen studied here is the positive $\Delta\varepsilon$, caused by the absence of large lateral dipole moments. This is a prerequisite for the splay FT in a planar cell, and it is essential for the electro-optic effects described here. Negative $\Delta\varepsilon$ (lateral molecular dipoles) may provide even better conditions to induce N_b since such nematics favor $\hat{n}$ perpendicular to $\vec{E}$. An electrical reorientation of the second director in a $\Delta\varepsilon<0$ material has been discussed, e.g., in [16]. In our samples, this effect is hidden by the reorientation of $\hat{n}_1$ in the electric field. Independent switching of the first and second directors in a biaxial nematic phase has been recently reported by Lee *et al.* [23]. However, we note that the authors of that paper use different models for their interpretation and come to very different conclusions. They obviously assume that, in the Fréedericksz transition, the director in the complete cell tilts uniformly. Since actually the director field above threshold is distorted, with zero deflection at the boundaries and maximum tilt in the cell middle [24], their model is apparently oversimplified and leads to misinterpretations of the optical character of the nematic material [25]. Moreover, they exclude biaxial clustering on the basis of handwaving arguments, and come to the conclusion that the electric field aligns the short axes of individual mesogens. This is in direct contrast to our model and conclusions.

ACKNOWLEDGMENTS

The authors acknowledge support by the DFG Grant No. STA 425/17.

[1] G. Pelzl, S. Diele, and W. Weissflog, Adv. Mater. **11**, 707 (1999); A. Eremin, H. Nadasi, G. Pelzl, S. Diele, H. Kresse, W. Weissflog, and S. Grande, Phys. Chem. Chem. Phys. **6**, 1290 (2004).

[2] M. W. Schröder, S. Diele, G. Pelzl, N. Pancenko, and W. Weissflog, Liq. Cryst. **29**, 1039 (2002).

[3] M. Hird, Liq. Cryst. Today **14**, 9 (2005).

[4] R. A. Reddy and C. Tschierske, J. Mater. Chem. **16**, 907 (2006).

[5] H. Takezoe and Y. Takanishi, Jpn. J. Appl. Phys., Part 1 **45**, 597 (2006).

[6] C. V. Yelamaggad, S. Krishna Prasad, G. G. Nair, I. S. Shashikala, D. S. Shankar Rao, C. V. Lobo, and S. Chandrasekhar, Angew. Chem. Int. Ed. **43**, 3429 (2004).

[7] M.-G. Tamba, B. Kosata, K. Pelz, S. Diele, G. Pelzl, Z. Vakovskaya, H. Kresse, and W. Weissflog, Soft Mater. **2**, 60 (2006).
[8] R. Amaranatha Reddy, M. W. Schröder, M. Bodyagin, H. Kresse, S. Diele, G. Pelzl, and W. Weissflog, Angew. Chem. **117**, 784 (2005); M. Nakata, R. F. Shao, J. E. Maclennan, W. Weissflog, and N. A. Clark, Phys. Rev. Lett. **96**, 067802 (2006).
[9] A. Eremin, S. Diele, G. Pelzl, and W. Weissflog, Phys. Rev. E **67**, 020702(R) (2003).
[10] W. Weissflog, M. W. Schröder, S. Diele, and G. Pelzl, Adv. Mater. (Weinheim, Ger.) **15**, 630 (2003); W. Weissflog, H. N. Shreenivasa Murthy, S. Diele, and G. Pelzl, Philos. Trans. R. Soc. London, Ser. A **364**, 2657 (2006).
[11] J. Harden, B. Mbanga, N. Éber, K. Fodor-Csorba, S. Sprunt, J. T. Gleeson, and A. Jákli, Phys. Rev. Lett. **97**, 157802 (2006); *e-lc communications* (2006) http://www.e-lc.org/docs/2006_07_18_08_47_15
[12] D. Wiant, J. T. Gleeson, N. Éber, K. Fodor-Csorba, A. Jákli, and T. Tóth-Katona, Phys. Rev. E **72**, 041712 (2005).
[13] R. Stannarius and J. Heuer, Eur. Phys. J. E **24**, 27 (2007).
[14] M.-G. Tamba, W. Weissflog, A. Eremin, J. Heuer, and R. Stannarius, Eur. Phys. J. E **22**, 85 (2007).
[15] L. J. Yu and A. Saupe, Phys. Rev. Lett. **45**, 1000 (1980).
[16] B. R. Acharya, A. Primak, and S. Kumar, Phys. Rev. Lett. **92**, 145506 (2004).
[17] L. A. Madsen, T. J. Dingemans, M. Nakata, and E. T. Samulski, Phys. Rev. Lett. **92**, 145505 (2004).
[18] G. R. Luckhurst, Nature (London) **430**, 413 (2004).
[19] H. Gruler and G. Meier, Mol. Cryst. Liq. Cryst. **16**, 299 (1972); H. Gruler, T. J. Scheffer, and G. Meier, Z. Naturforschung. **27A**, 966 (1972); H. Deuling, Mol. Cryst. Liq. Cryst. **19**, 123 (1972).
[20] L. Leger, Solid State Commun. **11**, 1499 (1972); F. Brochard, J. Phys. (France) **33**, 607 (1972).
[21] P. Toth, A. Buka, J. Peinke, and L. Kramer, Phys. Rev. E **58**, 1983 (1998); A. Buka, B. Dressel, W. Otowski, K. Camara, T. Toth-Katona, L. Kramer, J. Lindau, G. Pelzl, and W. Pesch, *ibid.* **66**, 051713 (2002).
[22] D. J. Photinos, Abstracts of the European Conference on Liquid Crystals, Lisbon, 2007; A. G. Vanakaras and D. J. Photinos, e-print arXiv:cond-mat/0707.3411.
[23] J.-H. Lee, T.-K. Lim, W.-T. Kim, and J-.I. Jin, J. Appl. Phys. **101**, 034105 (2007).
[24] See, e.g., A. Saupe, Z. Naturforsch. **15A**, 815 (1960); H. Deuling, Mol. Cryst. Liq. Cryst. **19**, 123 (1972); H. Gruler, T. J. Scheffer, and G. Meier, Z. Naturforsch. **27A**, 277 (1972).
[25] R. Stannarius (unpublished).
[26] The optical result $n_3 < n_2$ does not necessarily imply $\varepsilon_{33} < \varepsilon_{22}$, but it is the case here.